Hydroxylamine-induced oxidation of ferrous carbonylated truncated hemoglobins from Mycobacterium tuberculosis *and* Campylobacter jejuni *is limited by carbon monoxide dissociation*

Paolo Ascenzi, Chiara Ciaccio, Tecla Gasperi, Alessandra Pesce, Lucia Caporaso & Massimo Coletta

JBIC Journal of Biological Inorganic Chemistry

ISSN 0949-8257

J Biol Inorg Chem
DOI 10.1007/s00775-017-1476-x

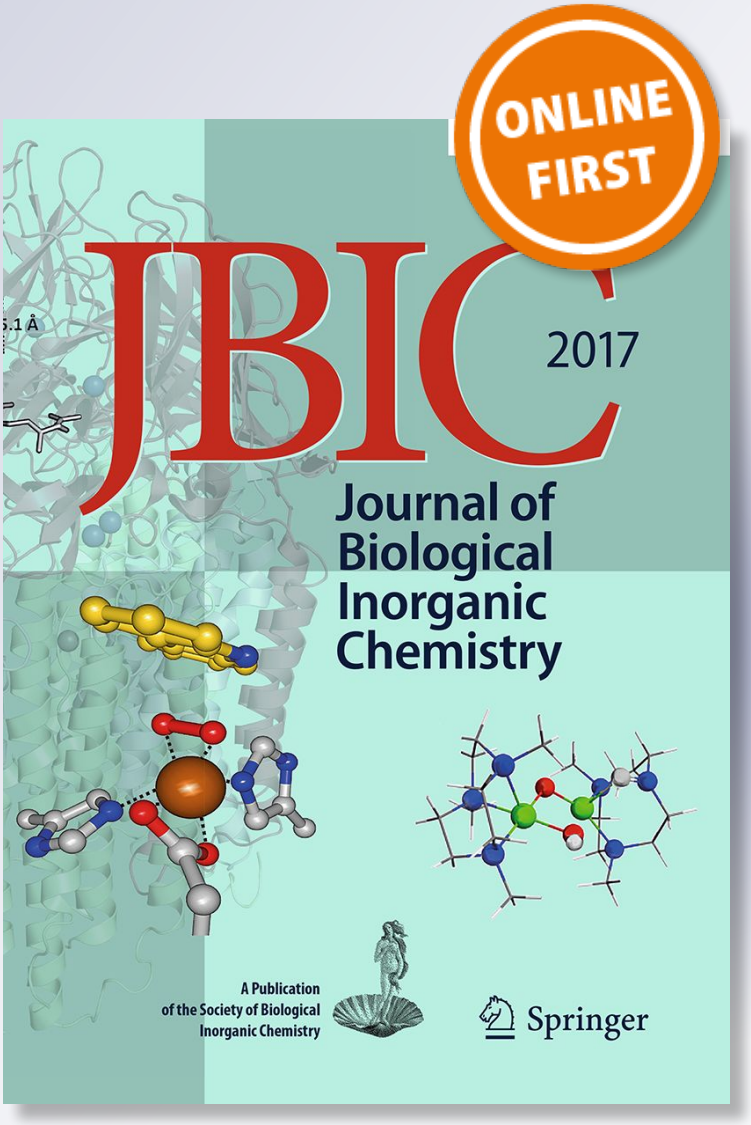

Springer

J Biol Inorg Chem
DOI 10.1007/s00775-017-1476-x

ORIGINAL PAPER

Hydroxylamine-induced oxidation of ferrous carbonylated truncated hemoglobins from *Mycobacterium tuberculosis* and *Campylobacter jejuni* is limited by carbon monoxide dissociation

Paolo Ascenzi[1] · Chiara Ciaccio[2,3] · Tecla Gasperi[4] · Alessandra Pesce[5] · Lucia Caporaso[6] · Massimo Coletta[2,3]

Received: 28 March 2017 / Accepted: 12 June 2017

Abstract Hydroxylamine (HA) is an oxidant of ferrous globins and its action has been reported to be inhibited by CO, even though this mechanism has not been clarified. Here, kinetics of the HA-mediated oxidation of ferrous carbonylated *Mycobacterium tuberculosis* truncated hemoglobin N and O (*Mt*-trHbN(II)-CO and *Mt*-trHbO(II)-CO, respectively) and *Campylobacter jejuni* truncated hemoglobin P (*Cj*-trHbP(II)-CO), at pH 7.2 and 20.0 °C, are reported. Mixing *Mt*-trHbN(II)-CO, *Mt*-trHbO(II)-CO, and *Cj*-trHbP(II)-CO solution with the HA solution brings about absorption spectral changes reflecting the disappearance of the ferrous carbonylated derivatives with the concomitant formation of the ferric species. HA oxidizes irreversibly *Mt*-trHbN(II)-CO, *Mt*-trHbO(II)-CO, and *Cj*-trHbP(II)-CO with the 1:2 stoichiometry. The dissociation of CO turns out to be the rate-limiting step for the oxidation of *Mt*-trHbN(II)-CO, *Mt*-trHbO(II)-CO, and *Cj*-trHbP(II)-CO by HA. Values of the second-order rate constant for HA-mediated oxidation of *Mt*-trHbN(II)-CO, *Mt*-trHbO(II)-CO, and *Cj*-trHbP(II)-CO range between 8.8×10^4 and 8.6×10^7 M^{-1} s^{-1}, reflecting different structural features of the heme distal pocket. This study (1) demonstrates that the inhibitory effect of CO is linked to the dissociation of this ligand, giving a functional basis to previous studies, (2) represents the first comparative investigation of the oxidation of ferrous carbonylated bacterial 2/2 globins belonging to the N, O, and P groups by HA, (3) casts light on the correlation between kinetics of HA-mediated oxidation and carbonylation of globins, and (4) focuses on structural determinants modulating the HA-induced oxidation process.

Keywords Truncated hemoglobin · Hydroxylamine · Oxidation · Kinetics

Abbreviations

Cj-trHbP	*Campylobacter jejuni* truncated hemoglobin P
Cj-trHbP(II)	Ferrous *Cj*-trHbP
Cj-trHbP(II)-CO	Carbonylated *Cj*-trHbP(II)
Cj-trHbP(III)	Ferric *Cj*-trHbP
HA	Hydroxylamine
Hb	Hemoglobin
Hb(II)	Ferrous Hb
Mb	Myoglobin
Mb(II)	Ferrous Mb
Mb(II)-CO	Carbonylated Mb(II)
Mt-trHbN	*Mycobacterium tuberculosis* truncated hemoglobin N
Mt-trHbN(II)	Ferrous *Mt*-trHbN
Mt-trHbN(II)-CO	Carbonylated *Mt*-trHbN(II)
Mt-trHbN(III)	Ferric *Mt*-trHbN
Mt-trHbO	*Mycobacterium tuberculosis* truncated hemoglobin O

✉ Paolo Ascenzi
ascenzi@uniroma3.it

1 Interdepartmental Laboratory for Electron Microscopy, Roma Tre University, 00146 Rome, Italy

2 Department of Clinical Sciences and Translational Medicine, University of Roma "Tor Vergata", 00133 Rome, Italy

3 Interuniversity Consortium for the Research on Chemistry of Metals in Biological Systems, 70126 Bari, Italy

4 Department of Sciences, Roma Tre University, 00146 Rome, Italy

5 Department of Physics, University of Genova, 16146 Genoa, Italy

6 Department of Mathematics and Physics, Roma Tre University, 00146 Rome, Italy

Published online: 23 June 2017

Mt-trHbO(II)	Ferrous *Mt*-trHbO
Mt-trHbO(II)-CO	Carbonylated *Mt*-trHbO(II)
Mt-trHbO(III)	Ferric *Mt*-trHbO
Ngb	Neuroglobin
Ngb(II)	Ferrous Ngb
trHb	Truncated Hb

Introduction

Globins, displaying either the 3-on-3 or the 2-on-2 α-helical fold, are present in all living organisms and are ordered in three lineages: (1) flavohemoglobins and single domain globins; (2) protoglobins and globin coupled sensors; and (3) truncated hemoglobins (trHb) [1–7]. They perform a wide range of essential biological functions including ligand transport, storage, and sensing, as well as heme-Fe-based catalysis [8–14].

Most of globin actions are impaired by the oxidation of the heme-Fe atom [8, 15, 16]. Indeed, the maintenance of hemoglobin (Hb) in the reduced form (heme-Fe(II)) in vivo depends primarily on two electron carriers, cytochrome b_5 and NADH, and the enzyme cytochrome b_5 reductase [17].

Among inorganic oxidizers, O_2, the physiological ligand of most globins, readily oxidizes heme-Fe(II) (3% of Hb is oxidized in 24 h), producing Hb-Fe(III) and the superoxide anion radical [8, 16]. Ferricyanide-mediated oxidation of ferrous oxygenated, carbonylated, and nitrosylated globins is preceded by O_2, CO, and NO dissociation [8, 18–20]. The oxidation of ferrous oxygenated and nitrosylated globins by NO and O_2, respectively, is characterized by the transient formation of the heme-Fe(III)-peroxynitrite complex preceding the release of NO_3^- [21–31]. Peroxynitrite oxidation of ferrous carbonylated globins is limited by the dissociation of CO, whereas the oxidation of the oxygenated derivative is characterized by the transient formation of an oxyferryl derivative preceding the formation of the ferric form. In contrast, peroxynitrite oxidizes ferrous nitrosylated globins via the transient formation of the ferric nitrosylated species that undergoes NO dissociation [30, 32–35]. The oxidation of ferrous globin derivatives by H_2O_2 involves the transient formation of the oxyferryl derivative, and then, an electron is transferred from the globin to the heme-Fe(IV)=O complex, resulting in peroxyl and/or phenoxyl radicals and the heme-Fe(III) atom [16, 30]. For all these reactions, the oxidant:heme-Fe(II) atom stoichiometry is 1:1 [8, 16–35]. In contrast, hydroxylamine (HA) oxidation of ligand-free ferrous globins, with the concomitant formation of ammonium, is characterized by the HA:heme-Fe(II) atom:ammonium stoichiometry 1:2:1; the reaction has been suggested to proceed via the geminate reduction mechanism [36–38]. The fast oxidation of hexa-coordinated ferrous plant Hbs by HA in comparison with penta-coordinated globins, displaying an intrinsic low affinity for HA, has been related to the weak hexa-coordination of the heme-Fe(II) atom by the His distal residue, which does not affect significantly the HA affinity. Moreover, the His distal side chain could contribute to the electron transfer reaction, and could be involved in catalysis [38]. Accordingly, the HA-mediated oxidation of hexa-coordinated ferrous human neuroglobin (Ngb(II)) is impaired by the tight heme-Fe(II)-His distal bond [38]. Moreover, the oxidation of ferrous globins by HA has been reported to be impaired by carbon monoxide and cyanide [36, 37].

The oxidation of ferrous carbonylated *Mycobacterium tuberculosis* trHbN (*Mt*-trHbN(II)-CO), *Mycobacterium tuberculosis* trHbO (*Mt*-trHbO(II)-CO), and *Campylobacter jejuni* trHbP (*Cj*-trHbP(II)-CO) by HA has been investigated to add further information to the intriguing reaction of HA with ferrous globins. This study has been dictated by the fact that HA has been reported to be involved in the nitrogen metabolism by ammonia-oxidizing bacteria [39–41]. Moreover, although no evidence for the involvement of trHbs in the metabolism of endogenous and exogenous CO has been reported, the high affinity of CO for trHbs [42–44] may cause not only hypoxemia, but it may impair heme-based chemistry by competitive binding to the ferrous metal center. Present data indicate that: (1) the heme-Fe atom:HA stoichiometry for the oxidation of *Mt*-trHbN(II)-CO, *Mt*-trHbO(II)-CO, and *Cj*-trHbP(II)-CO is 2:1; (2) the rate of oxidation of the heme-Fe(II) atom by HA is limited by CO dissociation; and (3) the values of the second-order rate constant for carbonylation and HA-mediated oxidation of ferrous globins are correlated and reflect the penta- and hexa-coordination of the heme-Fe atom.

Materials and methods

Mt-trHbN(III), *Mt*-trHbO(III), and *Cj*-trHbP(III) were cloned, expressed, and purified as previously reported [42, 45, 46]. The concentration of *Mt*-trHbN(III), *Mt*-trHbO(III), and *Cj*-trHbP(III) was determined spectrophotometrically at 406 nm ($\varepsilon = 1.4 \times 10^5$ M^{-1} cm^{-1}; pH 6.4), 409 nm ($\varepsilon = 1.0 \times 10^5$ M^{-1} cm^{-1}; pH 6.4), and 410 nm ($\varepsilon = 1.4 \times 10^5$ M^{-1} cm^{-1}; pH 6.4), respectively [47]. The trHb solutions were prepared dissolving the heme-proteins in 5.0×10^{-2} M phosphate buffer, pH 7.2, at 20.0 °C. The ferric derivatives were obtained by adding ferricyanide (final concentration, 2.0×10^{-3} M) to the trHb solutions [18]. Then, the ferric species were reduced to the ferrous derivatives by adding sodium dithionite (final concentration, 3.0×10^{-3} M). The excess of dithionite and by-products were removed by passing the protein solutions through a Sephadex G-10 gel filtration column (Amersham

Biosciences Europe GmbH, Freiburg, Germany) equilibrated in the air with 5.0×10^{-2} M phosphate buffer, pH 7.2, at 20.0 °C [18]. Then, the ferrous oxygenated trHbs solutions were gently degassed and the anaerobic CO solution (final concentration, 5.0×10^{-4} M) was added, under anaerobic conditions [18].

CO was purchased from Linde AG (Höllriegelskreuth, Germany). The CO solution was prepared by keeping in a closed vessel the 5.0×10^{-2} M phosphate buffer solution (pH = 7.2) under CO at $P = 760.0$ mmHg anaerobically (20.0 °C). The solubility of CO in the aqueous buffered solution is 1.03×10^{-3} M, at $P = 760.0$ mmHg and 20.0 °C [18].

All the other products (from Merck KGaA, Darmstadt, Germany) were of analytical grade and used without purification. The HA concentration was determined combining the oxidation of HA to nitrite by iodate ion in the acidic media and the nitrite determination by the acidic Griess reaction [48, 49].

The value of the first-order rate constant for the HA-induced conversion of ferrous carbonylated globins [Fe(II)-CO, i.e., *Mt*-trHbN(II)-CO, *Mt*-trHbO(II)-CO, and *Cj*-trHbP(II)-CO] to their ferric derivatives [Fe(III), i.e., *Mt*-trHbN(III), *Mt*-trHbO(III), and *Cj*-trHbP(III)] (i.e., k) was determined by mixing the Fe(II)-CO solutions (final concentration, ranging between 4.6×10^{-6} and 2.9×10^{-5} M) with the HA solution (final concentration, 4.0×10^{-5} to 2.0×10^{-4} M) under anaerobic conditions, at pH = 7.2 (5.0×10^{-2} M phosphate buffer) and 20.0 °C; no gaseous phase was present (see [19, 35]). Kinetics was monitored between 350 and 460 nm.

The time course of the HA-induced conversion of *Mt*-trHbN(II)-CO, *Mt*-trHbO(II)-CO, and *Cj*-trHbP(II)-CO to *Mt*-trHbN(III), *Mt*-trHbO(III), and *Cj*-trHbP(III), respectively, was fitted to a single or bi-phasic exponential process(es) according to the minimum reaction mechanism represented by Scheme 1 [37]. Kinetics reflects the competition of CO and HA for the metal center, which is controlled by the respective second-order association rate constant, namely, h' for CO and k_{on} for HA.

Values of the first-order rate constant for the HA-induced conversion of *Mt*-trHbN(II)-CO, and *Cj*-trHbP(II)-CO to *Mt*-trHbN(III) and *Cj*-trHbP(III), respectively (i.e., k) have been determined from data analysis, according to Eqs. (1) and (2):

$$[\text{Fe(II)}-\text{CO}]_t = [\text{Fe(II)}-\text{CO}]_i \times \left(1 - e^{-k \times t}\right), \quad (1)$$

$$[\text{Fe(II)}-\text{CO}]_t = [\text{Fe(II)}-\text{CO}]_i \times e^{-k \times t}, \quad (2)$$

depending on the observation wavelength.

Values of the first-order rate constant for the HA-induced conversion of *Mt*-trHbO(II)-CO to *Mt*-trHbO(III) (i.e., k_f *and* k_s) have been determined from data analysis, according to Eqs. (3) and (4):

$$[\text{Fe(II)}-\text{CO}]_t = [\text{Fe(II)}-\text{CO}]_i \times \left(Y_f \times \left(1 - e^{-k_f \times t}\right) + Y_s \times \left(1 - e^{-k_s \times t}\right)\right), \quad (3)$$

$$[\text{Fe(II)}-\text{CO}]_t = [\text{Fe(II)}-\text{CO}]_i \times \left(Y_f \times e^{-k_f \times t} + Y_s \times e^{-k_s \times t}\right), \quad (4)$$

where Y_f and Y_s indicate the molar fraction of the fast and slow reacting species, respectively.

Values of h and k_{on} have been determined from data analysis, according to Eq. (5):

$$k = (h \times ([\text{HA}]/[\text{CO}]))/\{(h \times H/k_{on}) + ([\text{HA}]/[\text{CO}])\}, \quad (5)$$

where H (= h'/h) is the association equilibrium constant for *Mt*-trHbN(II), *Mt*-trHbO(II), and *Cj*-trHbP(II) carbonylation [18, 42–44]. Equation (5) has been derived from Eq. (6) [18, 19]:

$$1/k = (H/k_{on}) \times [\text{CO}]/[\text{HA}] + 1/h. \quad (6)$$

Data were analyzed according to Eq. (5), since the linear representation of data (i.e., 1/k versus [CO]/[HA]) ignores the error contribution to the experimental data points leading to relative largely bias in the estimates of h and $h \times H/k_{on}$ values (see [50]).

It must be remarked that the plot of k as a function of [HA] (or of [HA]/[CO]), keeping constant $[\text{CO}] = 5.0 \times 10^{-4}$ M, displays a leveling off, since at high [HA] (whenever $[\text{HA}]/[\text{CO}] \gg h \times H/k_{on}$), Eq. (5) gives $k = h$.

$$2\text{Fe(II)-CO} + \text{HA} \underset{h'}{\overset{h}{\rightleftharpoons}} 2\text{Fe(II)} + 2\text{CO} + \text{HA} + 2\text{H}^+ \xrightarrow{k_{on}} 2\text{Fe(III)} + \text{NH}_4^+ + \text{OH}^-$$

Scheme 1 HA-mediated oxidation of ferrous carbonylated trHbs. h is the first-order rate constant for CO dissociation from Fe(II)-CO, h' is the second-order rate constant for CO association, and k_{on} is the second-order rate constant for the binding of hydroxylamine to Fe(II). k_{on} represents the rate-limiting step of the overall HA-mediated oxidation of Fe(II) to Fe(III) with the simultaneous reduction of HA to NH_4^+ [36–38]. HA indicates NH_2OH

On the other hand, according to Eq. (5), when $k = h/2$, we have that $h \times H/k_{on} = [HA]/[CO]$ from which the values of k_{on} have been obtained according to Eq. (7):

$$k_{on} = h \times H/R, \tag{7}$$

where R is the [HA]/[CO] value at $k = h/2$. Equation (7) has been solved accounting for either values of h and H obtained from the literature [42–44, 51] or of values of h calculated from fitting of data.

The results are given as mean values of at least four experiments plus or minus the corresponding standard deviation. All data were analyzed using programs Matlab (The Math Works Inc., Natick, MA, USA) and GraphPad Prism (GraphPad Software, San Diego, CA, USA).

Results and discussion

The HA-induced conversion of *Mt*-trHbN(II)-CO, *Mt*-trHbO(II)-CO, and *Cj*-trHbP(II)-CO to *Mt*-trHbN(III), *Mt*-trHbO(III), and *Cj*-trHbP(III), respectively, was investigated as a function of the HA concentration between 350 and 460 nm, at pH 7.2 and 20.0 °C. Difference absorption spectra shown in Figs. 1, 2, and 3 are much more informative than absolute absorption spectra allowing to put in evidence small variations, which would be missed only by looking at absolute absorption spectra.

Mixing the *Mt*-trHbN(II)-CO, *Mt*-trHbO(II)-CO, or *Cj*-trHbP(II)-CO solution with the HA solution brings about absorption spectral changes in the Soret band reflecting the disappearance of the ferrous carbonylated

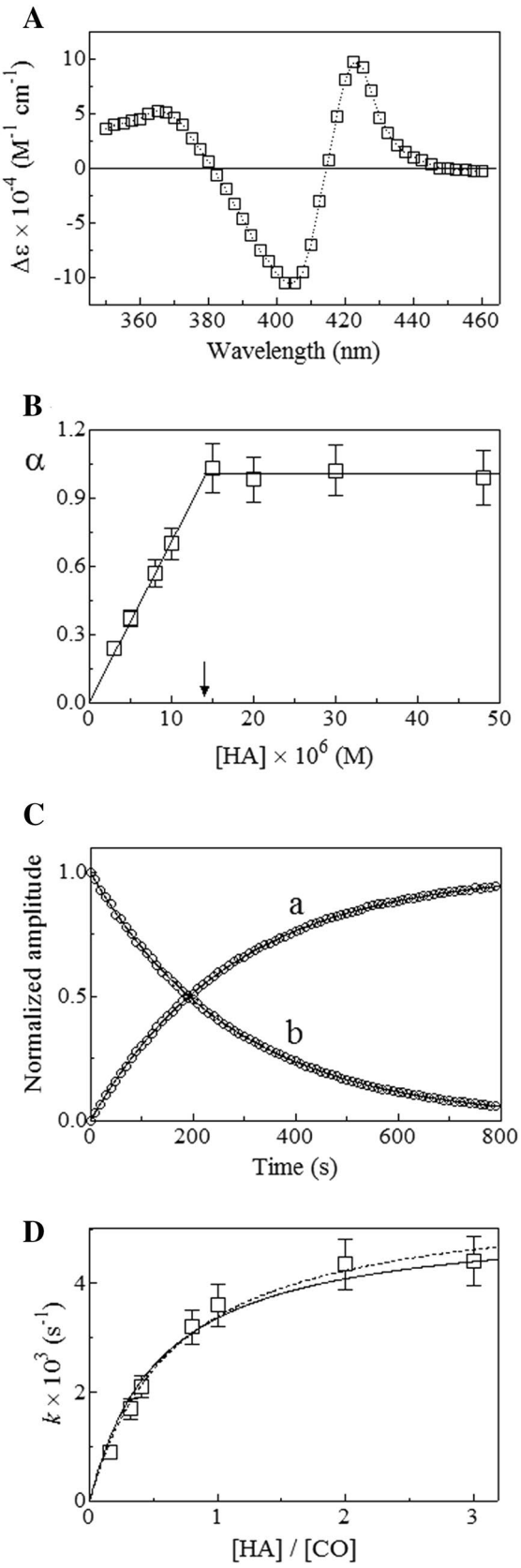

Fig. 1 Kinetics of HA-induced conversion of *Mt*-trHbN(II)-CO to *Mt*-trHbN(III). **a** Difference absorption spectrum of *Mt*-trHbN(II)-CO *minus* *Mt*-trHbN(III) obtained by mixing *Mt*-trHbN(II)-CO and HA solutions (*squares*). The *dotted line* indicates the difference absorption spectrum of *Mt*-trHbN(II)-CO *minus* *Mt*-trHbN(III) calculated from the absolute absorption spectra of *Mt*-trHbN(II)-CO and *Mt*-trHbO(III). **b** Dependence of the molar fraction of *Mt*-trHbN(III) (i.e., α) on the HA concentration. The *Mt*-trHbN(II)-CO concentration is 2.7×10^{-5} M. The [HA]:[*Mt*-trHbN(II)-CO] stoichiometry is 0.53:1.0 (*arrow*). **c** Normalized averaged time courses of the HA-induced conversion of *Mt*-trHbN(II)-CO to *Mt*-trHbN(III). The time courses were normalized at 406 nm (*trace a*) and 422 nm (*trace b*). The time course analysis according to Eqs. (1) (λ = 406 nm; *trace a*) and (2) (λ = 422 nm; *trace b*) allowed to determine the value of $k = 3.6 \times 10^{-3}$ s^{-1}. The HA concentration was 5.0×10^{-4} M. The [HA]/[CO] ratio was 1.0. **d** Dependence of k for the HA-induced conversion of *Mt*-trHbN(II)-CO to *Mt*-trHbN(III) on the [HA]/[CO] ratio. The *continuous* and *dashed lines* were calculated according to Eq. (5) with the following parameters: $h = 5.2 \times 10^{-3}$ s^{-1} (from [42, 51]) and $R = 0.55$, and $h = 5.6 \times 10^{-3}$ s^{-1} (present study) and $R = 0.66$, respectively. Where not shown, standard deviation is smaller than the symbol. For details, see text

derivatives with the concomitant formation of the ferric species (Figs. 1, 2, 3, panel A). The optical absorption spectra of ferrous carbonylated and ferric heme-proteins obtained here match very well with those reported in the literature (see Table 1) (see [18, 35, 42–44, 47, 52, 53]).

As shown in Figs. 1, 2, and 3 (panel B), HA catalyzes the conversion of *Mt*-trHbN(II)-CO, *Mt*-trHbO(II)-CO, and *Cj*-trHbP(II)-CO to *Mt*-trHbN(III), *Mt*-trHbO(III), and *Cj*-trHbP(III), respectively, with the 1:2 stoichiometry, as already reported for ferrous deoxygenated human Hb, horse heart Mb, rice non-symbiotic Hb, and *Synechocystis* Hb [36, 37]. This behavior corresponds to the reaction reported in Scheme 1 suggesting that for the overall process either the geminate or the dissociative mechanism could be operative (Scheme 2) [37]. On one hand, the geminate mechanism accounts for the delivery of two electrons to a single HA molecule, while it is bound to the same globin molecule. On the other hand, the dissociative mechanism would be characterized by a partially reduced HA species that dissociates from a heme-Fe(III) center and binds to another heme-Fe(II) species to trap the second electron (see Scheme 2).

No spectroscopic intermediates have been observed in the HA-mediated conversion of *Mt*-trHbN(II)-CO, *Mt*-trHbO(II)-CO, and *Cj*-trHbP(II)-CO to *Mt*-trHbN(III), *Mt*-trHbO(III), and *Cj*-trHbP(III), respectively (Figs. 1, 2, 3), although the E7 residue of *Mt*-trHbN is Leu [42].

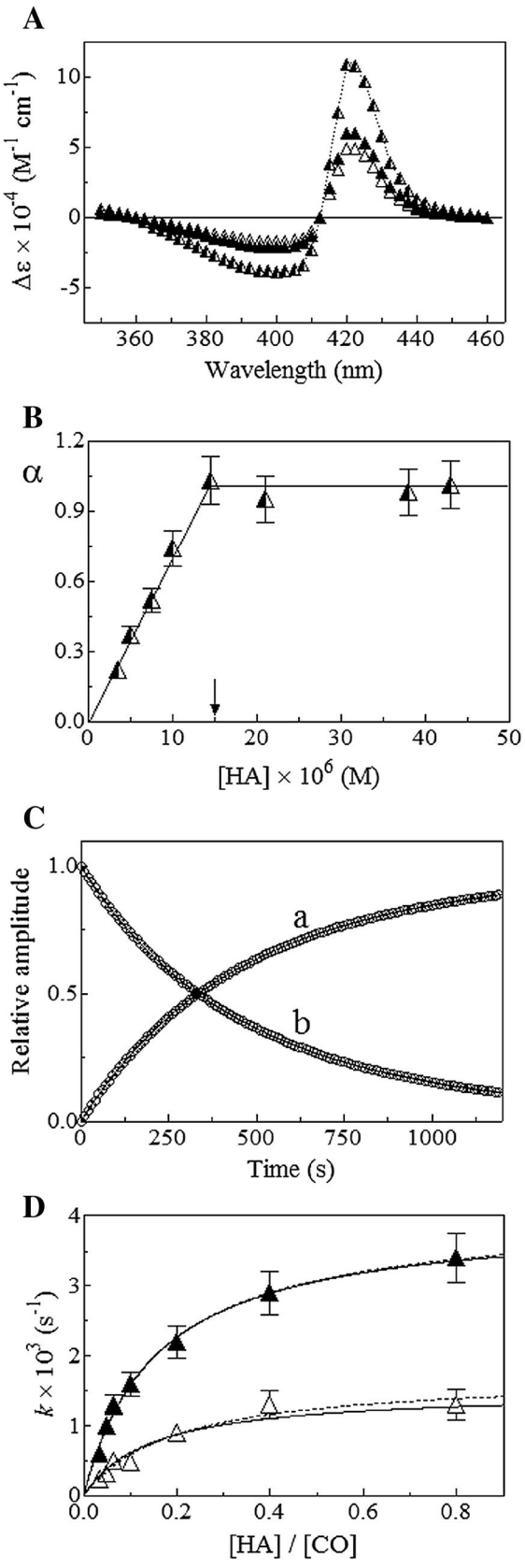

Fig. 2 Kinetics of HA-induced conversion of *Mt*-trHbO(II)-CO to *Mt*-trHbO(III) (fast phase, *filled triangles*; slow phase, *open triangles*). **a** Difference absorption spectrum of *Mt*-trHbO(II)-CO *minus Mt*-trHbO(III) obtained by mixing *Mt*-trHbO(II)-CO and HA solutions (*open-filled triangles*). The *filled* and *open triangles* indicate the difference absorption spectra of the fast and the slow phase, respectively, of *Mt*-trHbO(II)-CO *minus Mt*-trHbO(III). The *dotted line* indicates the difference absorption spectrum of *Mt*-trHbO(II)-CO *minus Mt*-trHbO(III) calculated from the absolute absorption spectra of *Mt*-trHbN(II)-CO and *Mt*-trHbO(III). **b** Dependence of the molar fraction of *Mt*-trHbO(III) (i.e., α) on the HA concentration. The *Mt*-trHbO(II)-CO concentration is 2.8×10^{-5} M. The [HA]:[*Mt*-trHbO(II)-CO] stoichiometry is 0.53:1.0 (arrow). **c** Normalized averaged time courses of the HA-induced conversion of *Mt*-trHbO(II)-CO to *Mt*-trHbO(III). The time courses were normalized at 408 nm (*trace a*) and 421 nm (*trace b*). The time course analysis according to Eqs. (3) ($\lambda = 408$ nm; *trace a*) and (4) ($\lambda = 421$ nm; *trace b*) allowed to determine the values of $k_f = 2.9 \times 10^{-3}$ s^{-1} and $k_s = 1.3 \times 10^{-3}$ s^{-1}. The values of Y_f and Y_s were 0.55 and 0.45, respectively. The HA concentration was 2.0×10^{-4} M. The [HA]/[CO] ratio was 4.0×10^{-1}. **d** Dependence of k for the HA-induced conversion of *Mt*-trHbO(II)-CO to *Mt*-trHbO(III) on the [HA]/[CO] concentration. The *continuous* and *dashed lines* were calculated according to Eq. (5) with the following parameters: slow phase: $h = 1.5 \times 10^{-3}$ s^{-1} (from [43]) and $R = 0.14$, and $h = 1.7 \times 10^{-3}$ s^{-1} (present study) and $R = 0.19$, respectively; fast phase: $h = 4.0 \times 10^{-3}$ s^{-1} (from [43]) and $R = 0.16$, and $h = 4.0 \times 10^{-3}$ s^{-1} (present study) and $R = 0.16$, respectively. For details, see text and Fig. 1

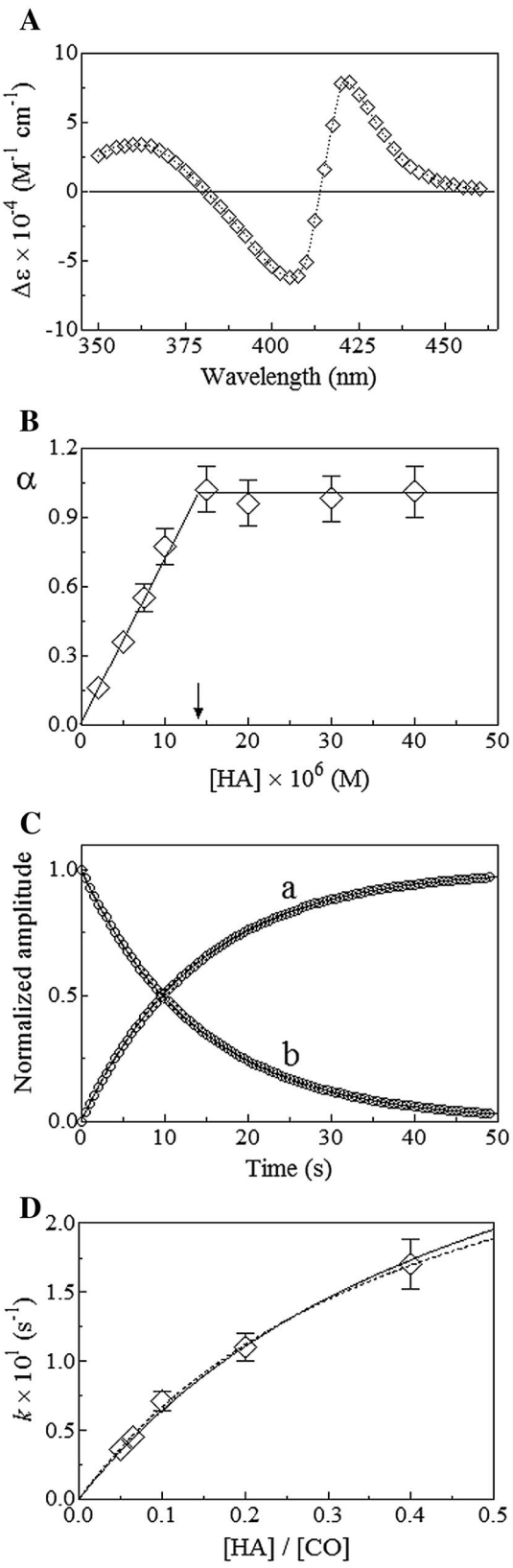

Fig. 3 Kinetics of HA-induced conversion of *Cj*-trHbP(II)-CO to *Cj*-trHbP(III). **a** Difference absorption spectrum of *Cj*-trHbP(II)-CO minus *Cj*-trHbP(III) obtained by mixing *Cj*-trHbP(II)-CO and HA solutions (*diamonds*). The *dotted line* indicates the difference absorption spectrum of *Cj*-trHbP(II)-CO minus *Cj*-trHbP(III) calculated from the absorbance absorption spectra of *Cj*-trHbP(II)-CO and *Cj*-trHbP(III). **b** Dependence of the molar fraction of Cj-trHbP(III) (i.e., α) on the HA concentration. The *Cj*-trHbP(II)-CO concentration is 2.9×10^{-5} M. The [HA]:[*Cj*-trHbP(II)-CO] stoichiometry is 0.48:1.0 (*arrow*). **c** Normalized averaged time courses of the HA-induced conversion of *Cj*-trHbP(II)-CO to *Cj*-trHbP(III). The time courses were normalized at 409 nm (*trace a*) and 420 nm (*trace b*). The time course analysis according to Eqs. (1) ($\lambda = 409$ nm; *trace a*) and (2) ($\lambda = 420$ nm; *trace b*) allowed to determine the value of $k = 7.1 \times 10^{-2}$ s^{-1}. The HA concentration was 5.0×10^{-5} M. The [HA]/[CO] ratio was 1.0×10^{-1}. **d** Dependence of k for the HA-induced conversion of *Cj*-trHbP(II)-CO to *Cj*-trHbP(III) on the [HA]/[CO] ratio. The *continuous* and *dashed lines* were calculated according to Eq. (5) with the following parameters: $h = 4.0 \times 10^{-1}$ s^{-1} (from [44]) and $R = 0.52$, and $h = 3.5 \times 10^{-1}$ s^{-1} (present study) and $R = 0.42$, respectively. For details, see text and Fig. 1

Indeed, the HisE7Leu mutant of non-symbiotic rice Hb undergoes transient spectral changes that reflect the occurrence of the short-lived heme-Fe(II)-HA complex [38]. The absence of spectroscopic intermediates is not an unexpected feature since the HA-mediated oxidation of carbonylated trHbs is rate-limited by CO dissociation.

The absence of spectroscopic intermediates suggests that: (1) the reaction could proceed via the geminate reduction mechanism, as proposed for the HA-catalyzed oxidation of ferrous deoxygenated human Hb, horse heart Mb, rice non-symbiotic Hb, and *Synechocystis* Hb [36, 37] and (2) the HA-induced oxidation of ferrous deoxygenated heme-proteins is very rapid compared to CO dissociation (see below). Although the dismutation of HA has been postulated (i.e., HA $\rightarrow N_2 + N_2O + NH_4^+$; the relative yields of oxidized and reduced products are expected to be either $N_2 + 2N_2O = NH_4^+$ or $N_2 \approx NH_4^+$ when N_2O is a minor product) [36], this reaction appears unlikely, since only ammonium has been detected as the final product of the HA-mediated oxidation of ferrous globins [37].

The time course of *Mt*-trHbN(II)-CO and *Cj*-trHbP(II)-CO oxidation by HA corresponds to a mono-exponential process (Figs. 1, 3, panel C). On the other hand, the time course of *Mt*-trHbO(II)-CO oxidation by HA is a bi-exponential process, the fast and the slow phases representing 55 ± 6 and $45 \pm 6\%$, respectively (Fig. 2, panel C); this bi-exponential behavior is in agreement with kinetics of O_2, CO, and NO binding to *Mt*-trHbO(II) [43] reflecting the existence of two different structural arrangements of the heme distal pocket in the ferrous ligated trHb [54].

Table 1 Values of λ_{max} and ε of the absorption spectra in the Soret region of ferric and ferrous carbonylated derivatives of *Mt*-trHbN, *Mt*-trHbO, and *Cj*-trHbP

Globin derivative	Present study[a]		From literature	
	λ_{max} (nm)	ε (M^{-1} cm^{-1})	λ_{max} (nm)	ε (M^{-1} cm^{-1})
Mt-trHbN(II)-CO	422	1.6×10^5	422[b]	1.5×10^{5b}
Mt-trHbN(III)	406	1.5×10^5	406[c]	1.4×10^{5c}
Mt-trHbO(II)-CO	421	1.8×10^5	421[d]	1.9×10^{5d}
Mt-trHbO(III)	408	1.1×10^5	409[c]	1.0×10^{5c}
Cj-trHbP(II)-CO	420	1.6×10^5	419[e]	1.5×10^{5e}
Cj-trHbP(III)	409	1.4×10^5	410[c,f]	$1.4 \times 10^{5c,f}$

[a] pH 7.2 and 20.0 °C

[b] pH 7.5 and 20.0 °C. Values were calculated from [42]

[c] pH 6.4 and 20.0 °C. From [47]

[d] pH 7.5 and 23.0 °C. Values were calculated from [43, 45]

[e] pH 7.0 and 20.0 °C. Values were calculated from [44, 52]

[f] pH 7.0 and 20.0 °C. From [44, 53]

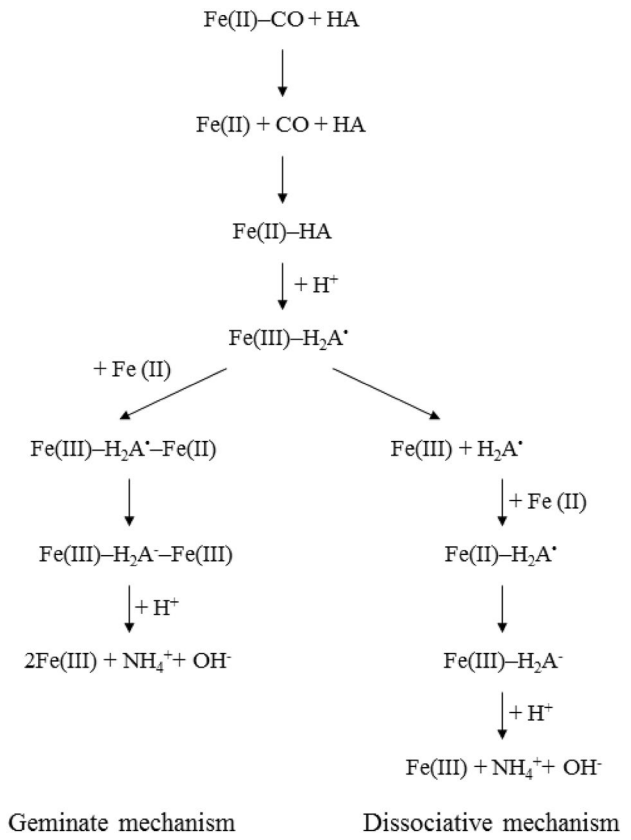

Scheme 2 Geminate and dissociative mechanisms for HA reduction to NH_4^+ by ferrous carbonylated trHbs. HA, $H_2A^•$, and H_2A^- indicate NH_2OH, H_2O–$^-NH_2$, and H_2O–$^-NH_2$, respectively. The symbol "–" does not indicate a covalent bond

Values of the first-order rate constant for *Mt*-trHbN(II)-CO, *Mt*-trHbO(II)-CO, and *Cj*-trHbP(II)-CO oxidation by HA (i.e., k) do not increase linearly with the HA concentration (i.e., [HA]), but tend to level off (Figs. 1, 2, 3, panel D). The analysis of data according to Eq. (5) allowed to determine the values of: (1) h under conditions, where the ratio [HA]/[CO] $\gg h \times H/k_{on}$ and (2) k_{on} when $k = h/2$ (see Eq. (7)).

Values of kinetic and/or thermodynamic parameters for *Mt*-trHbN(II)-CO, *Mt*-trHbO(II)-CO, *Cj*-trHbP(II)-CO, rice non-symbiotic Hb1(II), soybean Hb(II), tomato Hb(II), *Synechocystis* Hb(II), horse heart Mb(II), Ngb(II), and human Hb(II) oxidation by HA (i.e., k_{on}; present study and from [36–38]) and/or for heme-protein (de)carbonylation (i.e., h', h, and/or H) [18, 44, 51, 55–61] are summarized in Table 2.

As shown in Figs. 1, 2, and 3 (panel D), the conversion of *Mt*-trHbN(II)-CO, *Mt*-trHbO(II)-CO, and *Cj*-trHbP(II)-CO to *Mt*-trHbN(III), *Mt*-trHbO(III), and *Cj*-trHbP(III), respectively, catalyzed by HA is limited by a rate, whose value is represented by the asymptotic value of k (= h when [HA]/[CO] $\gg h \times H/k_{on}$, see Eq. 5), which turns out to be very close to that of CO dissociation from *Mt*-trHbN(II)-CO, *Mt*-trHbO(II)-CO, and *Cj*-trHbP(II)-CO taken from the literature [42–44] (i.e., h, see Table 2). This suggests that HA reacts only with penta-coordinated heme-Fe(II) atom (see also [38]), according to Scheme 1. Therefore, the observed inhibition of the HA-mediated oxidation of rice non-symbiotic Hb1(II), *Synechocystis* Hb(II), horse heart Mb(II), and human Hb(II) by CO [36, 37] may reflect the very low heme-Fe(II)-CO decarbonylation rate (i.e., h) representing the limiting step of the overall process.

An interesting relationship has been observed by plotting h' versus k_{on} (Fig. 4), indicating that kinetics of CO binding and of HA-mediated oxidation may be correlated according to the different structural features of the heme site and/or of the structural arrangement of the energetic barriers along the ligand pathway toward the heme pocket. However, it must be pointed out that both penta-coordinated horse heart Mb, human Hb, *Mt*-trHbN and *Cj*-trHbP and hexa-coordinated rice non-symbiotic Hb1, soybean Hb, and tomato Hb appear to fall on the same linear correlation, while the two forms of *Mt*-trHbO and human Ngb as well as *Synechocystis* Hb are outside. This suggests that different structural elements modulate the oxidation and ligand binding properties of the metal center.

In this respect, it must be remarked that all penta-coordinated heme-proteins (i.e., *Mt*-trHbN, *Cj*-trHbP, horse heart Mb, and human Hb) fall along the same correlation line (see Fig. 4), indeed indicating that kinetic determinants for the binding of CO [18, 42, 44, 61] and HA [36, 37] to the penta-coordinated heme-Fe(II) atom are similar. On the

Table 2 Kinetic parameters for HA-mediated oxidation and (de)carbonylation of ferrous heme-proteins

	HA	CO		
	k_{on} (M^{-1} s^{-1})	H[a] (M^{-1})	h' (M^{-1} s^{-1})	h (s^{-1})
Mt-trHbN(II)-CO	8.5×10^{6} [b]			5.6×10^{-3} [b]
				5.2×10^{-3} [c]
Mt-trHbN(II)		1.0×10^{9} [c]	5.3×10^{6} [c]	
Mt-trHbO(II)-CO	1.1×10^{6} [b]			1.7×10^{-3} (45%)[b]
				1.5×10^{-3} (40%)[d]
	8.8×10^{4} [b]			4.0×10^{-3} (55%)[b]
				4.0×10^{-3} (60%)[d]
Mb-trHbO(II)		1.2×10^{8} [d]	1.8×10^{5} (21%)[d]	
		3.5×10^{6} [d]	1.4×10^{4} (79%)[d]	
Cj-trHbP(II)-CO	8.6×10^{7} [b]			3.5×10^{-1} [b]
	1.8×10^{6} [b]			4.0×10^{-1} [e]
Cj-trHbP(II)		1.1×10^{8} [e]	4.5×10^{7} (15%)[e]	
		4.8×10^{6} [e]	1.9×10^{6} (85%)[e]	
Rice non-symbiotic Hb1(II)	2.5×10^{4} [f]		6.0×10^{6} [g]	
Soybean Hb(II)	~1.5×10^{5} [h]	1.6×10^{9} [i]	1.3×10^{7} [i]	7.8×10^{-3} [i]
Tomato Hb(II)	~7.5×10^{4} [h]	5.0×10^{7} [j]	1.0×10^{6} [j]	2.0×10^{-2} [j]
Synechocystis Hb(II)	2.8×10^{4} [f]		3.0×10^{5} [k]	
Horse heart Mb(II)	2.5×10^{2} [f]		5.0×10^{5} [l]	
Human Ngb(II)	~6.3×10^{2} [h]		~8.0×10^{3} [m]	
			~2.0×10^{3} [m]	
Human Hb(II)	3.0×10^{1} [n]		3.5×10^{5} [l]	
	1.1×10^{1} [n]		2.0×10^{5} [l]d	

[a] $H = h'/h$

[b] pH 7.2 and 20.0 °C. Present study

[c] pH 7.0 and 20.0 °C. From [42, 51]

[d] pH 7.5 and 23.0 °C. From [43]

[e] pH 7.0 and 20.0 °C. From [44]

[f] pH 7.0 and room temperature. From [37]

[g] pH 7.0; the temperature is not reported. From [55]

[h] pH 7.0; the temperature is not reported. From [38]

[i] pH 7.0 and 25.0 °C. From [58, 59]

[j] pH 7.0 and 25.0 °C. From [60]

[k] pH 7.0 and 20.0 °C. From [56, 57]

[l] pH 7.0 and 20.0 °C. From [18]

[m] pH 7.0 and 25.0 °C. From [61]

[n] pH 7.0 and 25.0 °C. From [36]

same correlation line, we find also the hexa-coordinated rice non-symbiotic Hb1, soybean Hb, and tomato Hb [37, 38] (Fig. 4), indicating that the energy of the sixth axial bond is fairly low and the dissociation of the endogenous ligand does not affect significantly the interaction of CO [55, 58–60] and HA [37, 38]. Indeed, the energy of the sixth axial bond in hexa-coordinated Hbs has been suggested to be an important factor in regulating HA reduction kinetics, such that a fast dissociating sixth ligand appears to even facilitate the HA reaction [38]. The intrinsically low affinity of HA for penta-coordinated globins has been highlighted by the low reactivity of the HisE7Leu mutant of rice non-symbiotic Hb [38]. However, the high reactivity of *Cj*-trHbP could reflect the in-plane geometry of the heme-Fe atom [53]. Moreover, the HA-mediated oxidation of ferrous hexa-coordinated human Ngb(II) is impaired by the tight coordination of the distal His residue to the heme-Fe(II) atom [38].

Somewhat different determinants must also come into play for the low-reactive hexa-coordinated heme-proteins, namely, *Mt*-trHbO, *Synechocystis* Hb, and human Ngb; thus, in these cases, the observed CO binding rate constants determined by rapid-mixing experiments [54, 56, 61] turn

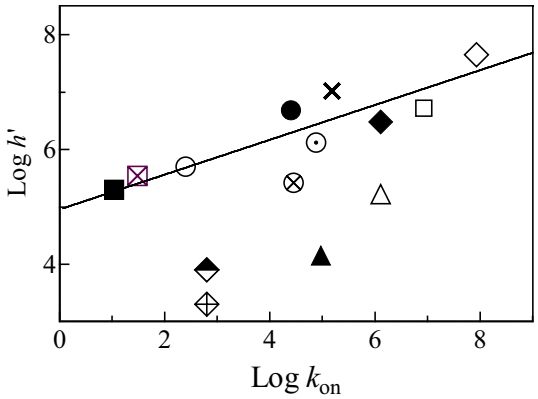

Fig. 4 Relationship between values of k_{on} for the HA-induced oxidation (M^{-1} s^{-1}) and of *h*' for carbonylation (M^{-1} s^{-1}) of *Mt*-trHbN (*square*), *Mt*-trHbO (*open* and *filled triangles*), *Cj*-trHbP (*open* and *filled diamonds*), rice non-symbiotic Hb1 (*filled circles*), soybean,Hb (*cross*), tomato Hb (*dotted circle*), *Synechocystis* Hb (*crossed circle*), horse heart Mb(II) (*open circle*), human Hb (*crossed* and *filled squares*), and human Ngb (*black-white* and *crossed diamonds*). The *continuous line* was calculated by linear regression of data referring to *Mt*-trHbN, *Cj*-trHbP, rice non-symbiotic Hb1, horse heart Mb, and human Hb. For details, see text

out to be much slower with respect to rice non-symbiotic Hb1 [55], in spite of closely similar (or even faster for one of the two forms of *Mt*-trHbO) HA association rate constants (present study and [37, 38]) (Fig. 4 and Table 2). This suggests that the lower CO reactivity of *Mt*-trHbO, *Synechocystis* Hb, and human Ngb with respect to HA (see Table 2), which positions them outside the linear correlation (Fig. 4), could be attributed to a higher bond energy for the hexa-coordinating ligand(s), which plays a major role for CO binding than for HA binding. This can be very well observed by comparing rice non-symbiotic Hb1 and the slow-reacting form of *Mt*-trHbO. In fact, these globins display a closely similar k_{on} value for the reaction with HA, but rice non-symbiotic Hb1 shows a 400-fold faster CO binding rate constant (i.e., *h*') (Fig. 4; Table 2).

Concluding remarks

The oxidation of ferrous heme-proteins by HA (present study and [36–38]) is reminiscent to that induced by ferricyanide [18, 19, 62] and peroxynitrite [35], although the globin:ferricyanide and :peroxynitrite stoichiometry is 1:1. Values of k_{on} for the oxidation of *Coryphaena hyppurus* Mb(II) by ferricyanide (1.2×10^7 M^{-1} s^{-1}) [19] and horse heart Mb(II) by peroxynitrite (~10^7 M^{-1} s^{-1}) [35] are similar to that observed for *Mt*-trHbN(II) oxidation by HA (8.5×10^6 M^{-1} s^{-1}; Table 2; present study). As reported here for the HA-induced oxidation of *Mt*-trHbN(II)-CO, *Mt*-trHbO(II)-CO, and *Cj*-trHbP(II)-CO (see Figs. 1, 2, 3), the oxidation of *Coryphaena hyppurus* Mb(II)-CO and horse heart Mb(II)-CO by ferricyanide is limited by CO dissociation [19, 20, 35], clearly indicating that the oxidation takes place in the penta-coordinated species and requires the dissociation of the hexa-coordinating ligand of the heme-Fe atom.

In conclusion, this investigation has demonstrated that, like for the oxidation of the heme-Fe(II) atom induced by ferricyanide and peroxynitrite, the hydroxylamine-induced oxidation requires a penta-coordinated metal center, being rate-limited by the dissociation of an exogenous ligand. This evidence explains the inhibitory effect exerted by CO on the oxidation of human Hb, horse heart Mb, rice non-symbiotic Hb1, and *Synechocystis* Hb by HA [36, 37]. In particular, it must be pointed out that in penta-coordinated species, the structural determinants of CO binding and HA-induced oxidation appear to be essentially the same, as indicated by the linear correlation between the second-order rate constants of HA and CO association. However, in the case of the hexa-coordinated *Mt*-trHbO and *Synecocystis* Hb, the bond strength of the hexa-coordinating endogenous ligand seems to play a larger role for CO binding ($\Delta \mathrm{Log}h'$ ~2.7; Fig. 4) than for the HA-induced oxidation rate ($\Delta \mathrm{Log}k_{on}$ ~1; Fig. 4), indeed suggesting that the redox ligand-linked equilibrium might be regulated in a different fashion, eventually including electron transfer pathways within the protein matrix [63]. It should be pointed out that in the case of *Mt*-trHbO, the hexa-coordinating ligand is not His but TyrB10 or TyrCD1 [54] and this may affect the HA reduction rates, as suggested for plant Hbs [38].

As a whole, this investigation indicates that in penta-coordinated heme-proteins, the electron transfer occurs preferentially (though not uniquely) through the direct interaction of the electron donor (or acceptor) with the metal center, requiring the dissociation of any exogenous ligand. Conversely, in the case of heme-proteins, where an endogenous ligand axially coordinates the heme-Fe atom, a different strategy seems to have been developed, allowing the same electron donor (or acceptor) to efficiently transfer electrons through alternative pathways, which need to be identified.

Acknowledgements This work was partially supported by a grant (CAL 2016 to PA) from Roma Tre University (Rome, Italy).

References

1. Vinogradov SN, Hoogewijs D, Bailly X, Arredondo-Peter R, Guertin M, Gough J, Dewilde S, Moens L, Vanfleteren JR (2005) Proc Natl Acad Sci USA 102:11385–11389
2. Vuletich DA, Lecomte JTJ (2006) J Mol Evol 62:196–210
3. Vinogradov SN, Hoogewijs D, Bailly X, Arredondo-Peter R, Gough J, Dewilde S, Moens L, Vanfleteren JR (2006) BMC Evol Biol 6:31

4. Ascenzi P, Bolognesi M, Milani M, Guertin M, Visca P (2007) Gene 398:42–51
5. Vinogradov SN, Hoogewijs D, Bailly X, Mizuguchi K, Dewilde S, Moens L, Vanfleteren JR (2007) Gene 398:132–142
6. Vinogradov SN, Moens L (2008) J Biol Chem 283:8773–8777
7. Vinogradov SN, Bailly X, Smith DR, Tinajero-Trejo M, Poole RK, Hoogewijs D (2013) Adv Microb Physiol 63:391–446
8. Bunn HF, Forget BG (1986) Hemoglobin: molecular, genetic and clinical aspects. WB Saunders Company, Philadelphia
9. Bolognesi M, Bordo D, Rizzi M, Tarricone C, Ascenzi P (1997) Prog Biophys Mol Biol 68:29–68
10. Wittenberg JB, Bolognesi M, Wittenberg BA, Guertin M (2002) J Biol Chem 277:871–874
11. Smith LJ, Kahraman A, Thornton JM (2010) Proteins 78:2349–2368
12. Pesce A, Bolognesi M, Nardini M (2013) Adv Microb Physiol 63:49–78
13. Pesce A, Bolognesi M, Nardini M (2013) Adv Microb Physiol 63:79–96
14. Ascenzi P, Brunori M (2016) J Porphyrins Phthalocyanines 29:1–16
15. Mansouri A, Lurie AA (1993) Am J Hematol 42:7–12
16. Rifkind JM, Ramasamy S, Manoharan PT, Nagababu E, Mohanty JG (2004) Antioxid Redox Signal 6:657–666
17. Elahian F, Sepehrizadeh Z, Moghimi B, Mirzaei SA (2014) Crit Rev Biotechnol 34:134–143
18. Antonini E, Brunori M (1971) Hemoglobin and myoglobin in their reactions with ligands. North-Holland Publishing Co, Amsterdam
19. Bannister JV, Bannister WH, Ascenzi P, Focesi A, Brunori M (1976) FEBS Lett 65:361–364
20. Ascenzi P, Petrella G, Coletta M (2007) Biochem Biophys Res Commun 359:871–876
21. Herold S (1999) FEBS Lett 443:81–84
22. Minning DM, Gow AJ, Bonaventura J, Braun R, Dewhirst M, Goldberg DE, Stamler JS (1999) Nature 401:497–502
23. Herold S, Exner M, Nauser T (2001) Biochemistry 40:3385–3395
24. Herold S, Fago A, Weber RE, Dewilde S, Moens L (2004) J Biol Chem 279:22841–22847
25. Møller JKS, Skibsted LH (2004) Chem Eur J 10:2291–2300
26. Herold S, Puppo A (2005) J Biol Inorg Chem 10:935–945
27. Herold S, Röck G (2005) Biochemistry 44:6223–6231
28. Fasano M, Antonini G, Ascenzi P (2006) Biochem Biophys Res Commun 345:704–712
29. Ascenzi P, Bolognesi M, Visca P (2007) Biochem Biophys Res Commun 357:809–814
30. De Marinis E, Casella L, Ciaccio C, Coletta M, Visca P, Ascenzi P (2009) IUBMB Life 61:62–73
31. Koebke KJ, Pauly DJ, Lerner L, Liu X, Pacheco AA (2013) Inorg Chem 52:7623–7632
32. Exner M, Herold S (2000) Chem Res Toxicol 13:287–293
33. Ascenzi P, Milani M, Visca P (2006) Biochem Biophys Res Commun 351:528–533
34. Herold S, Boccini F (2006) Inorg Chem 45:6933–6943
35. Ascenzi P, Ciaccio C, Coletta M (2007) Biochem Biophys Res Commun 363:931–936
36. Bazylinski DA, Arkowitz RA, Hollocher TC (1987) Arch Biochem Biophys 259:520–526
37. Sturms R, DiSpirito AA, Fulton DB, Hargrove MS (2011) Biochemistry 50:10829–10835
38. Athwal SN, Alagurajan J, Andreotti AH, Hargrove MS (2016) Biochemistry 55:5809–5817
39. Ferguson SJ (1998) Curr Opin Chem Biol 2:182–193
40. Stein LY (2011) Methods Enzymol 486:131–152
41. Kozlowski JA, Kits KD, Stein LY (2016) Front Microbiol 7:1090
42. Couture M, Yeh S, Wittenberg BA, Wittenberg JB, Ouellet Y, Rousseau DL, Guertin M (1999) Proc Natl Acad Sci USA 96:11223–11228
43. Ouellet H, Juszczak L, Dantsker D, Samuni U, Ouellet YH, Savard PY, Wittenberg JB, Wittenberg BA, Friedman JM, Guertin M (2003) Biochemistry 42:5764–5774
44. Farrés J, Rechsteiner MP, Herold S, Frey AD, Kallio PT (2005) Biochemistry 44:4125–4134
45. Mukai M, Savard PY, Ouellet H, Guertin M, Yeh SR (2002) Biochemistry 41:3897–3905
46. Nardini M, Pesce A, Labarre M, Richard C, Bolli A, Ascenzi P, Guertin M, Bolognesi M (2006) J Biol Chem 281:37803–37812
47. Ascenzi P, di Masi A, Tundo GR, Pesce A, Visca P, Coletta M (2014) PLoS One 9:e102811
48. Miranda KM, Espey MG, Wink DA (2001) Nitric Oxide 5:62–71
49. Afkhami A, Madrakian T, Maleki A (2005) Anal Biochem 347:162–164
50. Malatesta F, Ascenzi P (1993) Biochem Mol Biol Educ 23:88
51. Ascenzi P, Coletta A, Cao Y, Trezza V, Leboffe L, Fanali G, Fasano M, Pesce A, Ciaccio C, Marini S, Coletta M (2013) PLoS One 8:e69762
52. Lu C, Egawa T, Wainwright LM, Poole RK, Yeh SR (2007) J Biol Chem 282:13627–13636
53. Bolli A, Ciaccio C, Coletta M, Nardini M, Bolognesi M, Pesce A, Guertin M, Visca P, Ascenzi P (2008) FEBS J 275:633–645
54. Mukai M, Savard PY, Ouellet H, Guertin M, Yeh SR (2002) Biochemistry 41:3897–3905
55. Hargrove MS (2000) Biophys J 79:2733–2738
56. Hvitved AN, Trent JT 3rd, Premer SA, Hargrove MS (2001) J Biol Chem 276:34714–34721
57. Hoy JA, Smagghe BJ, Halder P, Hargrove MS (2007) Protein Sci 16:250–260
58. Appleby CA (1969) Biochim Biophys Acta 1188:222–229
59. Gibson QH, Wittenberg JB, Wittenberg BA, Bogusz D, Appleby CA (1989) J Biol Chem 264:100–107
60. Ioanitescu AI, Dewilde S, Kiger L, Marden MC, Moens L, Van Doorslaer S (2005) Biophys J 89:2628–2639
61. Fago A, Mathews AJ, Dewilde S, Moens L, Brittain T (2006) J Inorg Biochem 100:1339–1343
62. Coletta M, Santucci R, Focesi A Jr, Ascoli F, Brunori M (1987) Biochim Biophys Acta 915:415–419
63. Weiland T, Kundu S, Trent J, Hoy J, Hargrove M (2004) J Am Chem Soc 126:11930–11935